methods

Alternative splicing attenuates transgenic expression directed by the apolipoprotein E promoter-enhancer based expression vector pLIV11[S]

Dongmei Cheng, Philip S. MacArthur, Shunxing Rong, John S. Parks, and Gregory S. Shelness[1]

Department of Pathology, Section on Lipid Sciences, Wake Forest University School of Medicine, Winston Salem, NC 27157

Abstract The plasmid vector pLIV11 is used commonly to achieve liver-specific expression of genes of interest in transgenic mice and rabbits. Expression is driven by the human apolipoprotein (apo)E 5′ proximal promoter, which includes 5 kb of upstream sequence, exon 1, intron 1, and 5 bp of exon 2. A 3.8 kb 3′ hepatic control region, derived from a region ~18 kb downstream of the apoE gene, enhances liver-specific expression. Here, we report that cDNA sequences inserted into the multiple cloning site (MCS) of pLIV11, which is positioned just downstream of truncated exon 2, can cause exon 2 skipping. Hence, splicing is displaced to downstream cryptic 3′ splice acceptor sites causing deletion of cloned 5′ untranslated mRNA sequences and, in some cases, deletion of the 5′ end of an open reading frame. To prevent use of cryptic splice sites, the pLIV11 vector was modified with an engineered 3′ splice acceptor site inserted immediately downstream of truncated apoE exon 2. Presence of this sequence fully shifted splicing of exon 1 from the native intron 1–exon 2 splice acceptor site to the engineered site. This finding confirmed that sequences inserted into the MCS of the vector pLIV11 can affect exon 2 recognition and provides a strategy to protect cloned sequences from alternative splicing and possible attenuation of transgenic expression.—Cheng, D., P. S. MacArthur, S. Rong, J. S. Parks, and G. S. Shelness. **Alternative splicing attenuates transgenic expression directed by the apolipoprotein E promoter-enhancer based expression vector pLIV11. *J. Lipid Res.* 2010.** 51: **849–855.**

Supplementary key words exon skipping • liver-specific transgenic expression • microsomal triglyceride transfer protein • RNA processing • transgenic mice

Apolipoprotein (apo)E is expressed most abundantly in the liver, although low expression is also observed in many nonhepatic tissues, including brain and kidney. Simonet et al. (1) identified a 3′ distal hepatic control region (HCR) responsible for directing high levels of hepatocyte-specific expression of apoE and silencing of apoE in nonhepatic tissues, including kidney. On this basis, expression plasmids were designed that contained the 5′ proximal promoter region (which also included noncoding exon 1, intron 1, and 5 bp of exon 2), a multiple cloning site (MCS) for inserting genes of interest, part of exon 4 (which contains a polyadenylation site), and the 3.8 kb HCR (**Fig. 1A**). This vector, pLIV11, as well as the related plasmid, pLIVLE6, which contains a subdomain of the 3.8 kb HCR, have been successfully used to achieve high levels of expression of a number of genes of interest in both transgenic mouse (2–8) and rabbit (9) liver.

In the current report, the pLIV11 vector was employed to express the *Drosophila* and human orthologs of MTP (10–12). We report that sequences cloned within the MCS of pLIV11 can affect 3′ splice acceptor site selection during removal of intron 1, resulting in exon 2 skipping and deletion of 5′ segments of mRNA. A method of protecting cloned sequences from use as cryptic splice acceptor sites was developed.

MATERIALS AND METHODS

Plasmid construction and generation of transgenic mice

Plasmids pLIV11 (1) and pLIV11-Not1 (7) were obtained from Liqing Yu, Wake Forest University School of Medicine. pLIV11-Not1 is a derivative of pLIV11 containing additional rare restriction sites, including NotI, positioned at the 5′ end of the

This work was supported by National Institutes of Health Grants HL049373 (G.S.S. and J.S.P.) and HL054176 (J.S.P.) P.M. was supported by National Institutes of Health Training Grant T-32 HL091797. Its contents are solely the responsibility of the authors and do not necessarily represent the official views of the National Institutes of Health.

Manuscript received 28 September 2009 and in revised form 27 October 2009.

Published, JLR Papers in Press, October 27, 2009
DOI 10.1194/jlr.D002709

Abbreviations: dMTP, *Drosophila* microsomal triglyceride transfer protein; HCR, hepatic control region; hMTP, human microsomal triglyceride transfer protein; MCS, multiple cloning site.

[1] To whom correspondence should be addressed.
e-mail: gshelnes@wfubmc.edu

[S] The online version of this article (available at http://www.jlr.org) contains supplementary data in the form of five figures and one table.

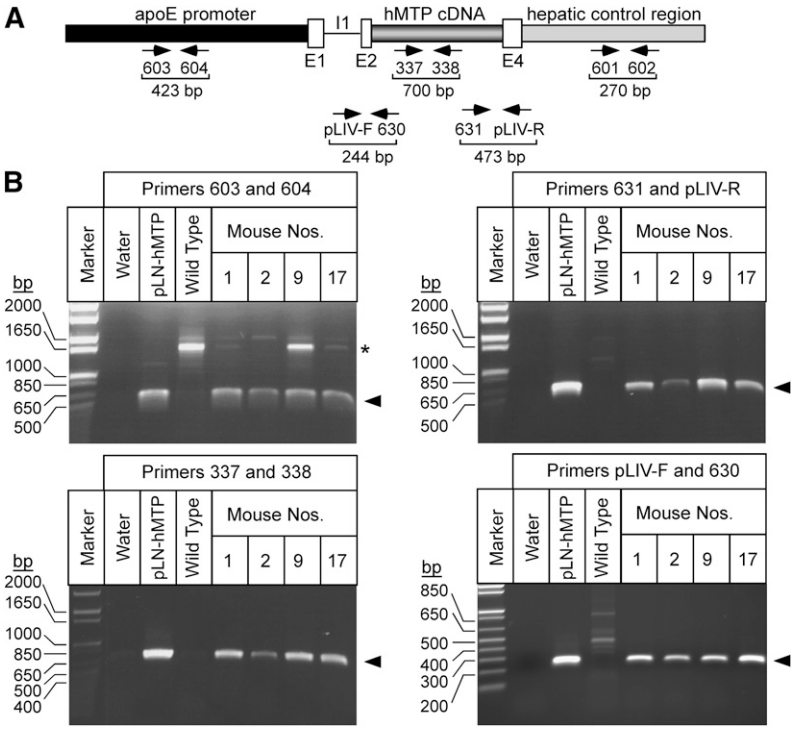

Fig. 1. Genotypic characterization of hMTP transgenic mice. A: Organization of hMTP cloned into pLIV11-NotI (E, exon; I, intron). Arrows indicate approximate position of PCR primers used for genotyping; amplicon sizes, in bp, are indicated for each primer pair (supplementary Table I). B: The indicated primer sets were used to amplify tail DNA from wild-type mice and transgenic founders 1, 2, 9, and 17. PCR of water serves as a negative control and PCR of plasmid pLN-hMTP serves as a positive control. Arrowheads indicate position of expected PCR products; asterisk indicates a nonspecific band.

transgenic cassette to facilitate separation of the transgene from the plasmid backbone.

Inserting human MTP (hMTP) cDNA into pLIV11-NotI. The 5′ end of the hMTP cDNA insert was released from plasmid pRC/neo (13) by digestion with SpeI, followed by treatment with T4 DNA polymerase. The 3′ end was released by digestion with MluI. pLIV11-NotI was digested with ClaI followed by treatment with T4 DNA polymerase. Linearized plasmid was digested with MluI and dephosphorylated with calf intestine alkaline phosphatase. Following gel purification, the hMTP insert and pLIV11-NotI plasmid were ligated and transformed into *Escherichia coli* strain XL1-Blue. The resulting plasmid is named pLN-hMTP.

Inserting Drosophila MTP cDNA (dMTP) into pLIV11-NotI. The dMTP cDNA insert was separated from plasmid pCMV5 (10) by digestion with *Eco*RI (5′ end) and ClaI (3′ end), followed by treatment with T4 DNA polymerase. pLIV11-NotI was digested with HpaI and dephosphorylated with calf intestine alkaline phosphatase. Following gel purification, the dMTP insert and pLIV11-NotI plasmid were ligated and transformed into *E. coli* XL1-Blue. The resulting plasmid is named pLN-dMTP.

Inserting mouse LCAT (mLCAT) cDNA into pLIV11. mLCAT sequence was amplified from mouse liver cDNA using the forward primer, mLCAT tg1F (5′-TACCAATTGTGTGATGGGGCTGCCTGGCT- 3′) and the reverse primer, mLCAT tg1R (5′-AGTACGCGTTTATTCAGGGGGTGGGGGACT-3′). The PCR product was digested with the primer-encoded restriction enzymes, MfeI (forward primer) and MluI (reverse primer). pLIV11 was digested with MfeI and MluI. Following gel purification, the mLCAT insert and pLIV11 plasmid were ligated and transformed into *E. coli* DH5α. The resulting plasmid is named pL-mLCAT.

The entire insert and flanking regions of each plasmid construct were verified by sequence analysis. The pLN-hMTP and -dMTP transgenes were separated from the plasmid backbone by digestion with NotI (5′) and SpeI (3′); pL-mLCAT was digested with SalI (5′) and SpeI (3′). Following isolation by agarose gel electrophoresis, transgenic cassettes were microinjected into pronuclei of fertilized C57BL/6 (Harlan Teklad) eggs by the Transgenic Mouse Core Facility of Wake Forest University. All mice were housed in a pathogen–free animal facility in plastic cages in a temperature-controlled room (22°C) with a 12-h light and 12-h dark cycle. The mice were fed ad libitum a cereal-based rodent chow diet. All animal procedures were conducted in conformity with Public Health Service policy and were approved by the Institutional Animal Care and Use Committee of Wake Forest University School of Medicine.

RNA purification and RT-PCR

RNA was isolated from frozen liver or cells by homogenization in TRIzol, as recommended by the manufacturer (Invitrogen). RNA was treated with DNase I using TURBO DNA-free KIT (Applied Biosystems; AM1907). Reverse transcription was performed in a final volume of 40 µl containing 4 µg of RNA, 500 µM dNTPs, 20 U RNase inhibitor, 200 ng random hexamer primers (Promega) and 8 U of Omniscript reverse transcriptase (Qiagen). Samples were incubated at 37°C for 60 min followed by denaturation at 95°C for 5 min. PCR was performed in 50 µl reactions containing 2 µl of reverse transcriptase reaction, 50 ng each of forward and reverse primer, 200 µM dNTP, 1× GoTaq buffer (Promega), 1.5 mM $MgCl_2$, and 0.5 µl (2.5 U) of Taq DNA polymerase (GoTaq; Promega). Reactions were incubated at 94°C for 2 min followed by 39 cycles as follows: 94°C, 1 min 15 s; 55°C, 1 min; 72°C, 1 min.

Sequencing of PCR products

PCR products were separated by agarose gel electrophoresis, excised from the gel, and purified using QiaQuick columns according to the supplier's protocol (Qiagen). PCR products were sequenced by the Biomolecular Resource Laboratory of the Comprehensive Cancer Center of Wake Forest University using an Applied Biosystems Model 3100 Genetic Analyzer.

Generation of anti-human MTP antiserum

cDNA corresponding to amino acid residues 772-874 of hMTP (precursor protein) was generated by PCR and cloned

into the vector pMAL-c2× (New England Biolabs) for generation in *E. coli* of a maltose binding protein-hMTP fusion protein. Following purification via amylose affinity chromatography, the fusion protein was injected subcutaneously into rabbits with incomplete Freund's adjuvant (Lampire Biologicals, Pipersville, PA). Whole serum was used at 1:1000 dilution for immunoblot analysis.

RESULTS

Generation of hMTP transgenic mice

Initial PCR analyses of tail DNA from pLN-hMTP transgenic founders using primers specific for the 3′ HCR (601 and 602; supplementary Table I; supplementary Fig. I), revealed that four of 18 mice harbored one or more copies of the transgene. Subsequent PCR analyses using primers specific for the 5′ proximal promoter, the hMTP insert, and the 5′ and 3′ vector-insert junctions demonstrated integration of the intact transgene (Fig. 1). The four genotypically positive founders were bred with wild-type C57BL/6 mice; however, only pLN-hMTP founders 1 and 17 produced genotypically positive offspring. Immunoblot analysis of liver extracts from founders 1 and 17 offspring failed to produce an immunoreactive band, although the anti-hMTP antibody (supplementary Fig. II) did react with African green monkey liver extract and extracts from human hepatoma cells (HepG2 and HuH-7; **Fig. 2A**, upper). When the blot was stripped and reprobed with a monoclonal antibody specific for mouse MTP, bands were detected in mouse liver and McA-RH7777 (rat hepatoma) extracts, although not in African green monkey liver or human hepatoma cell extracts (Fig. 2A, lower). These data indicate that despite the presence of the transgene, hMTP expression was undetectable in offspring from two genotypically positive hMTP transgenic founders.

Transgenic hMTP mRNA contains 5′ deletions

To explore whether mRNA transcribed from the transgene was present and of the predicted structure, pLN-hMTP founder 1 liver mRNA was subjected to RT-PCR using primers that spanned the entire transcription unit. Four of the primer pairs gave rise to RT-PCR products of the expected size (Fig. 2B, Lanes 2–5); however primer set 659+651, which spans apoE intron 1 (Fig. 1C), gave rise to a band of ∼700 bp rather than the expected 918 bp (Fig. 2B, Lane 1). Hence, although the transgene was transcribed, the 5′ end of the predominant mRNA species appeared aberrant. To explore the structure of the mRNA further, the 659+651 PCR product was sequenced using antisense primer 668 (supplementary Table I and Fig. 2C). The sequence evident from the electropherogram is homogenous until the region defined by the 90 degree arrow in supplementary Fig. IIIA. At this point, two sequences appear, neither of which corresponds to the expected product. Identical PCR sizes and sequences (data not shown) were observed using liver RNA from pLN-hMTP founder 17. To determine if generation of the heterogeneous hMTP mRNA sequences was unique to expression in transgenic mouse liver or inherent to the construct, pLN-hMTP was transfected into HepG2 cells and RNA was

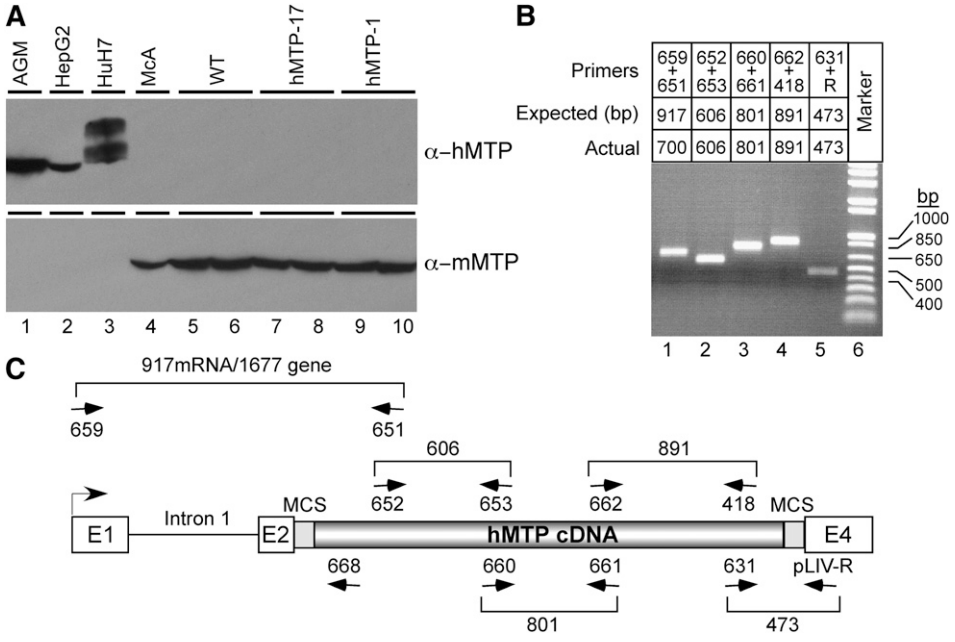

Fig. 2. hMTP expression in transgenic mice. A: Immunoblot of wild-type (WT), and hMTP-1 and -17 transgenic mice using anti-human MTP antibody (α-hMTP; supplementary Fig. II). Also analyzed are African green monkey liver (AGM), HepG2, HuH-7 (human hepatoma), and McA-RH7777 (McA; rat hepatoma) cell extracts. The upper blot was stripped and probed with anti-mouse MTP antibody (lower; α-mMTP; BD, Material number 612022). B: RT-PCR was performed using RNA from hMTP-1 mouse liver as template and indicated primers (supplementary Table I; R, pLiv-R). The expected and actual sizes of RT-PCR products are given. C: Relative position of primer pairs used for RT-PCR in Panel B (MCS, multiple cloning site).

subjected to RT-PCR and sequence analysis, as described for supplementary Fig. IIIA. As observed in supplementary Fig. IIIB, the sequences obtained were identical to those observed in transgenic mice. Based on these results, it appears that when expressed in either mouse liver or transfected hepatoma cells, the pLN-hMTP plasmid gives rise to three mRNA sequences. Sequence 1 is the expected, although the least abundant sequence. Sequences 1A and 1B are the predominant species and each contain extensive deletions (**Fig. 3**).

Transgenic hMTP mRNA 5′ deletions arise due to alternative splicing

The nature of the deletions observed in transgenic mouse liver and transfected HepG2 cells was consistent with alternative splicing, as each of the deletions occurred 3′ of AG dinucleotides, which were preceded by pyrimidine-rich domains (14) (Fig. 3). The sites of putative alternative splicing, involving removal of introns 1A and 1B, are diagrammed in **Fig. 4A**. These two splicing events, which give rise to the majority of mature mRNA, involved removal of the initiating ATG, thereby producing a dysfunctional transcript. Although the properly spliced species is rare, such that it is barely visible in the sequencing electropherograms in supplementary Fig. IIIA and B, it can be detected by RT-PCR using the appropriate primer pair (primers 667 and 668; supplementary Table I), as observed in Fig. 4B, lanes 10–12. However, this species is present in trace abundance, as evidenced by the inability to detect the mRNA without performing high cycle number PCR using primers 659 and 668, which can detect each of the three sequences (Fig. 4B, lane 4) and the fact that the protein product was undetectable in transgenic mouse liver (Fig. 2A).

A possible explanation for the preferential use of the downstream cryptic 3′ splice acceptor sites in pLN-hMTP is that the native intron 1–exon 2 junction underwent mutagenesis. As specified under Material and Methods, the starting pLN-hMTP plasmid was sequenced, including exon 1, intron 1, and exon 2. The apoE-derived plasmid

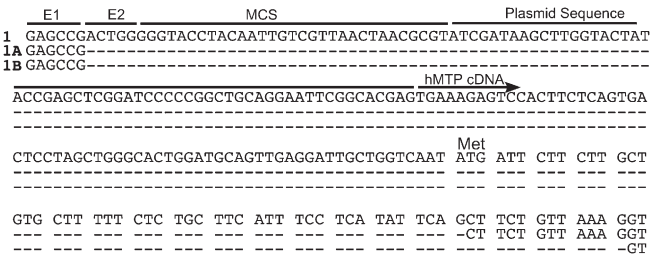

Fig. 3. hMTP mRNA sequence heterogeneity in mouse liver and transfected HepG2 cells. RNA from transgenic founder 1 liver or pLN-hMTP-transfected HepG2 cells (FuGENE HD; Roche) was subjected to RT-PCR using primers 659 and 651 and sequencing using antisense primer 668 (supplementary Table I and Fig. 2C). The multiple sequences observed in the electropherograms (supplementary Fig. IIIA, B) are depicted. E1 and E2, exons 1 and 2; MCS, multiple cloning sequence; Plasmid Sequence is sequence derived from the original hMTP expression plasmid that was carried over into pLN-hMTP; dashes indicate deleted nucleotides; arrow indicates beginning of hMTP cDNA.

sequence was identical to the published apoE gene sequence used to assemble this plasmid (15) as well corresponding database entries (e.g., locus NW_001838496). To ensure that mutations affecting the 3′ splice acceptor site did not occur during generation of transgenic mice, the appropriate region of transgenic mouse tail DNA was amplified by PCR with primers 659 and 630 and then sequenced with oligo 630 (supplementary Table I, Figs. 1A, 2C). The 573 nucleotide sequence starting at exon 2 and extending upstream into intron 1 was also identical to the published sequence (data not shown), indicating that no mutation within or proximal to the 3′ splice acceptor site was responsible for the observed alternative splicing.

A consensus 3′ splice acceptor site positioned downstream of the apoE intron 1–exon 2 border blocks activation of cryptic splice sites within hMTP cDNA

In an attempt to protect the cDNA sequences cloned into pLIV11-NotI from being used as cryptic 3′ splice acceptor sites during intron 1 removal, the pLN-hMTP plasmid was modified to encode an engineered 3′ splice acceptor site positioned downstream of the native intron 1–exon 2 junction but upstream of the hMTP cDNA to form plasmid pLNSR-hMTP (**Fig. 5A**). When this construct was transfected into HepG2 cells and RNA subjected to RT-PCR with primers 659 and 668, a PCR product size of ~400 bp was observed (Fig. 5B, lane 5), consistent with splicing at the engineered splice acceptor site. In contrast, both pLN-hMTP-transfected HepG2 cell and transgenic mouse liver RNA gave products of ~260 bp, consistent with splicing at the alternative sites (Fig. 5B, lanes 3, 4). Sequence analysis of the pLNSR-hMTP RT-PCR product revealed a homogenous sequence, consistent with splicing of exon 1 to the engineered splice acceptor site 1 (Fig. 5A) and retention of the initiating ATG codon (supplementary Fig. IV and data not shown). Hence, the presence of the engineered 3′ splice acceptor site fully shifted exon 1 splicing from the native intron 1–exon 2 junction to the new site and prevented use of the downstream cryptic splice sites diagrammed in Fig. 4A. These results confirm that sequences cloned downstream of truncated exon 2 can dramatically affect native intron 1, 3′ splice acceptor site utilization and also provides a strategy for protecting cloned sequences from undergoing deletion via alternative splicing. To this end, pLIV11-NotI was modified to contain the engineered 3′ splice acceptor site by ligating the same double stranded oligonucleotide shown in Fig. 5A into the MunI and MluI sites of pLIV11-Not1 to form the variant plasmid, pLIV11-NSR (Fig. 5C). cDNA sequences cloned into the MluI and/or ClaI sites of this vector should not be subjected to alternative splicing even if they contain cryptic 3′ splice acceptor sites.

Other cloned sequences promote alternative splicing in pLIV11

In contrast to our experience with hMTP, the vector pLIV11 has been used widely and successfully to achieve transgenic expression of a variety of genes. We attribute this to one of two possibilities: *1*) the sequences cloned

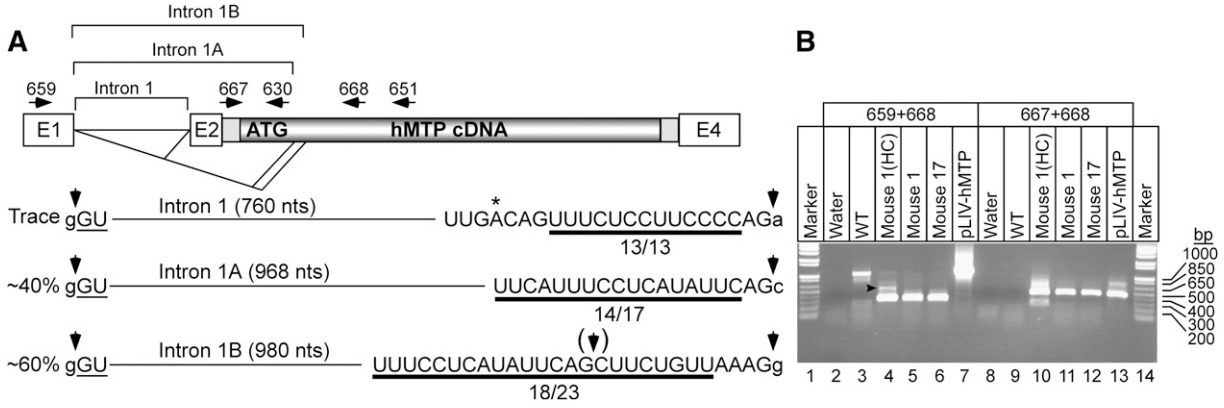

Fig. 4. Alternative splicing of transgenic hMTP. A: Intron–exon structure of the hMTP transgene is depicted. Brackets and diagonal lines define introns utilized during hMTP mRNA processing. Intron 1 is the native apoE intron; introns 1A and 1B arise from skipping of exon 2 and utilization of downstream cryptic 3′ splice acceptor sites. The sequence details found at the native and alternative 3′ splice acceptor sites are shown. The vertical arrows indicate the intron boundaries (lower case is used for exonic sequence). The underlined sequence shows the pyrimidine rich track, which precedes the AG dinucleotide at the 3′ end of the introns; the numbers indicate the number of pyrimidines/number of total nucleotides within the underlined region. The intron 1A and 1B splice acceptor sites are closely spaced; hence, the parenthetic arrow in the intron 1B sequence defines the splice acceptor site utilized for formation of intron 1A. B: RT-PCR of hMTP mouse liver RNA using the indicated primers. Primer pair 667 and 668 is specific for the properly spliced mRNA product generated by removal of native intron 1; primer pair 659 and 668 amplify all of the splicing products (arrowhead indicates PCR product corresponding to removal of native apoE intron 1); the predominant products corresponding to removal of introns 1A and 1B are similarly sized and run as a single band. HC, high cycle PCR generated by isolating initial PCR products and subjecting to a second round of PCR. Lanes 7 and 13 show PCR results using pLIV-hMTP plasmid as template with the indicated primers.

into the vector contain either no or very weak cryptic splice acceptor sites or in some other way do not negatively affect apoE intron 1–exon 2 splice site recognition, or *2*) alternative splicing is taking place but removes only 5′ untranslated sequences, leaving the open reading frame intact. To explore the generality of our observations regarding alternative splicing, we analyzed mRNA from NPC1L1 (7), mLCAT, and dMTP transgenic mice. Using primers that sequence from the 3′ to 5′ end of the transgenic mRNAs, we noted no signs of alternative splicing in NPC1L1 transgenic mouse liver (data not shown). In contrast, dMTP and mLCAT mice both showed signs of alternative splicing. In the case of dMTP, the alternative splicing occurred upstream of the initiating ATG codon; in the case of mLCAT, alternative splicing occurred within the open reading frame, although this was a minor product (supplementary Fig. V).

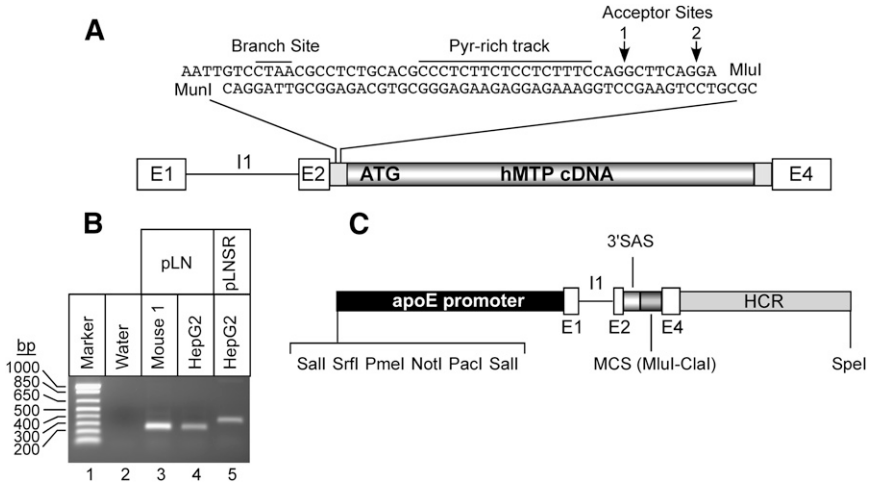

Fig. 5. Insertion of an engineered 3′ splice acceptor site protects hMTP from alternative splicing. A: A double stranded oligonucleotide containing an engineered 3′ splice acceptor site was inserted into pLN-hMTP at the MunI and MluI sites, as indicated, to form plasmid pLNSR-hMTP. The branch site, pyrimidine (Pyr)-rich track, and predicted splice acceptor sites are indicated. B: pLN-hMTP (pLN) and pLNSR-hMTP (pLNSR) were transfected into HepG2 cells using FuGENE HD. RNA from transfected cells and from founder 1 (Mouse 1) liver was subjected to RT-PCR using primers 659 and 668, as described for Fig. 4B, and sized by agarose gel electrophoresis. C: Organization of vector pLIV11-NSR. Restriction enzyme sites at the 5′ and 3′ ends appropriate for separating transgene from plasmid backbone are shown (note that SalI appears twice). The 3′ splice acceptor site (3′SAS) shown in A, was cloned into the MunI and MluI sites of pLIV11-NotI, leaving MluI and ClaI for inserting cDNAs of interest.

DISCUSSION

The 5′ proximal promoter elements as well as the 3′ HCR are critical to drive high levels of liver-specific expression using the vector pLIV11 and its derivatives. The exon 1–intron 1–exon 2 sequences present in this construct may also be important as in some studies, intronic sequences were shown to increase transgenic expression (16). In the current report, we demonstrated that sequences cloned downstream of the intron 1–exon 2 splice acceptor site can affect splice site utilization, resulting in exon 2 skipping and use of cryptic splice acceptor sites located within a cloned cDNA. In the case of pLN-hMTP, splicing resulted in deletion of an initiating codon and failed transgenic expression.

The reason for the poor utilization of the native apoE intron 1, 3′ splice acceptor site is uncertain. For the most part, the *cis*-acting sequences that drive splice site selection are contained within introns themselves, which are recognized by components of the spliceosome (14, 17). In particular, 3′ splice acceptor sites adhere to a consensus that includes a conserved A positioned ~18–50 nucleotides upstream of the 3′ end of the intron, which serves a branch point for lariat formation, a ⩾11 nucleotide pyrimidine-rich tract, and a conserved AG dinucleotide (18–20). Based on its close adherence to the consensus sequence, the native apoE intron 1, 3′ splice acceptor site would be expected to serve as an efficient substrate. Indeed, based on database searches and available literature, no evidence of alternative splicing involving human apoE exon 2 was found. Nonetheless, alternative splicing is a common means of achieving protein diversity and is believed to affect ~40–60% of human genes (21). Alternative splicing is driven in part by the presence of splicing enhancer and silencing elements, some of which are encoded within exonic sequences (17, 22–26). In this regard, several studies report that truncations of internal exons can dramatically affect 3′ splice site utilization. For example, progressive 3′ - 5′ truncation of an internal exon in the human β-globin gene from 171 to either 23, 29, or 33 nucleotides, resulted in quantitative exon skipping (27). Although small exons exist in nature, these are usually flanked by strong intronic splicing enhancers (28). We propose, therefore, that truncation of apoE exon 2 from its native 66 nucleotide length to the 5 nucleotides present in pLIV11 could affect splice site selection by either loss of an exonic splice enhancer or, more likely, because sequences that replace the truncated exon (in this case cDNA) either negatively affect splice site selection at the native site or enhance utilization of a downstream cryptic site.

As a means to protect cloned sequences from alternative splicing, an engineered 3′ splice acceptor site was inserted downstream of the native apoE intron1–exon 2 junction in pLIV11 (Fig. 5A). Presence of this sequence resulted in a complete shift of splicing to the engineered site, confirming the weak context of the native splice acceptor site contained within pLIV11 and providing a means to prevent opportunistic use of downstream cryptic splice acceptor sites contained within cDNA. This modification to the pLIV11 plasmid and its derivative seems advisable to ensure unattenuated expression of cloned sequences. Accordingly, for future use, a variant of pLIV11-NotI termed pLIV11-NSR was engineered as diagrammed in Fig. 5C.

Alternatively, should unmodified pLIV11 vector be employed for transgenic expression, cDNA sequences should be screened and, if possible, modified to remove potential cryptic 3′ splice acceptor sites. Although the large size of pLIV11-related plasmids gives rise to low transfection efficiencies, making detection of protein overexpression in cultured cells difficult, the use of RT-PCR revealed that the pattern of splicing in mouse liver and HepG2 cells was identical (supplementary Fig. III). Hence, the sizing and sequence analyses of RT-PCR products derived from pLIV11-transfected HepG2 or other hepatoma cells can provide a reliable means of monitoring the pattern of splicing and mRNA structure prior to oocyte injection.

The authors thank Liqing Yu, M.D, Ph.D. for plasmids pLIV11 and pLIV11-NotI and for valuable advice.

REFERENCES

1. Simonet, W. S., N. Bucay, S. J. Lauer, and J. M. Taylor. 1993. A far-downstream hepatocyte-specific control region directs expression of the linked human apolipoprotein E and C–I genes in transgenic mice. *J. Biol. Chem.* **268:** 8221–8229.
2. Yamanaka, S., M. E. Balestra, L. D. Ferrell, J. L. Fan, K. S. Arnold, S. Taylor, J. M. Taylor, and T. L. Innerarity. 1995. Apolipoprotein B mRNA-editing protein induces hepatocellular carcinoma and dysplasia in transgenic animals. *Proc. Natl. Acad. Sci. USA.* **92:** 8483–8487.
3. Allan, C. M., and J. M. Taylor. 1996. Expression of a novel human apolipoprotein (apoC-IV) causes hypertriglyceridemia in transgenic mice. *J. Lipid Res.* **37:** 1510–1518.
4. Engelking, L. J., H. Kuriyama, R. E. Hammer, J. D. Horton, M. S. Brown, J. L. Goldstein, and G. Liang. 2004. Overexpression of Insig-1 in the livers of transgenic mice inhibits SREBP processing and reduces insulin-stimulated lipogenesis. *J. Clin. Invest.* **113:** 1168–1175.
5. Schneider, M., J. L. Witztum, S. G. Young, E. H. Ludwig, E. R. Miller, S. Tsimikas, L. K. Curtiss, S. M. Marcovina, J. M. Taylor, R. M. Lawn, et al. 2005. High-level lipoprotein [a] expression in transgenic mice: evidence for oxidized phospholipids in lipoprotein [a] but not in low density lipoproteins. *J. Lipid Res.* **46:** 769–778.
6. Monetti, M., M. C. Levin, M. J. Watt, M. P. Sajan, S. Marmor, B. K. Hubbard, R. D. Stevens, J. R. Bain, C. B. Newgard, R. V. Farese, Sr., et al. 2007. Dissociation of hepatic steatosis and insulin resistance in mice overexpressing DGAT in the liver. *Cell Metab.* **6:** 69–78.
7. Temel, R. E., W. Tang, Y. Ma, L. L. Rudel, M. C. Willingham, Y. A. Ioannou, J. P. Davies, L-M. Nilsson, and L. Yu. 2007. Hepatic Niemann-Pick C1-like 1 regulates biliary cholesterol concentration and is a target of ezetimibe. *J. Clin. Invest.* **117:** 1968–1978.
8. Vaisman, B. L., G. Lambert, M. Amar, C. Joyce, T. Ito, R. D. Shamburek, W. J. Cain, J. Fruchart-Najib, E. D. Neufeld, A. T. Remaley, H. B. Brewer, Jr., and S. Santamarina-Fojo. 2001. ABCA1 overexpression leads to hyperalphalipoproteinemia and increased biliary cholesterol excretion in transgenic mice. *J. Clin. Invest.* **108:** 303–309.
9. Fan, J., J. Wang, A. Bensadoun, S. J. Lauer, Q. Dang, R. W. Mahley, and J. M. Taylor. 1994. Overexpression of hepatic lipase in transgenic rabbits leads to a marked reduction of plasma high density lipoproteins and intermediate density lipoproteins. *Proc. Natl. Acad. Sci. USA.* **91:** 8724–8728.

10. Sellers, J. A., L. Hou, H. Athar, M. M. Hussain, and G. S. Shelness. 2003. A Drosophila microsomal triglyceride transfer protein homolog promotes the assembly and secretion of human apolipoprotein B. Implications for human and insect lipid transport and metabolism. *J. Biol. Chem.* **278:** 20367–20373.
11. Shelness, G. S., and A. S. Ledford. 2005. Evolution and mechanism of apolipoprotein B-containing lipoprotein assembly. *Curr. Opin. Lipidol.* **16:** 325–332.
12. Rava, P., G. K. Ojakian, G. S. Shelness, and M. M. Hussain. 2006. Phospholipid transfer activity of microsomal triacylglycerol transfer protein is sufficient for the assembly and secretion of apolipoprotein B lipoproteins. *J. Biol. Chem.* **281:** 11019–11027.
13. Gordon, D. A., H. Jamil, D. Sharp, D. Mullaney, Z. Yao, R. E. Gregg, and J. Wetterau. 1994. Secretion of apolipoprotein B-containing lipoproteins from HeLa cells is dependent on expression of the microsomal triglyceride transfer protein and is regulated by lipid availability. *Proc. Natl. Acad. Sci. USA.* **91:** 7628–7632.
14. Black, D. L. 2003. Mechanisms of alternative pre-messenger RNA splicing. *Annu. Rev. Biochem.* **72:** 291–336.
15. Paik, Y. K., D. J. Chang, C. A. Reardon, G. E. Davies, R. W. Mahley, and J. M. Taylor. 1985. Nucleotide sequence and structure of the human apolipoprotein E gene. *Proc. Natl. Acad. Sci. USA.* **82:** 3445–3449.
16. Choi, T., M. Huang, C. Gorman, and R. Jaenisch. 1991. A generic intron increases gene expression in transgenic mice. *Mol. Cell. Biol.* **11:** 3070–3074.
17. Chen, M., and J. L. Manley. 2009. Mechanisms of alternative splicing regulation: insights from molecular and genomics approaches. *Nat. Rev. Mol. Cell Biol.* **10:** 741–754.
18. Mount, S. M. 1982. A catalogue of splice junction sequences. *Nucleic Acids Res.* **10:** 459–472.
19. Ruskin, B., A. R. Krainer, T. Maniatis, and M. R. Green. 1984. Excision of an intact intron as a novel lariat structure during pre-mRNA splicing in vitro. *Cell.* **38:** 317–331.
20. Reed, R., and T. Maniatis. 1985. Intron sequences involved in lariat formation during pre-mRNA splicing. *Cell.* **41:** 95–105.
21. Modrek, B., and C. Lee. 2002. A genomic view of alternative splicing. *Nat. Genet.* **30:** 13–19.
22. Watakabe, A., K. Tanaka, and Y. Shimura. 1993. The role of exon sequences in splice site selection. *Genes Dev.* **7:** 407–418.
23. Cartegni, L., S. L. Chew, and A. R. Krainer. 2002. Listening to silence and understanding nonsense: exonic mutations that affect splicing. *Nat. Rev. Genet.* **3:** 285–298.
24. Ladd, A., and T. Cooper. 2002. Finding signals that regulate alternative splicing in the post-genomic era. *Genome Biol.* **3**: reviews0008.0001–reviews0008.0016.
25. Zheng, Z-M. 2004. Regulation of alternative RNA splicing by exon definition and exon sequences in viral and mammalian gene expression. *J. Biomed. Sci.* **11:** 278–294.
26. Goren, A., O. Ram, M. Amit, H. Keren, G. Lev-Maor, I. Vig, T. Pupko, and G. Ast. 2006. Comparative analysis identifies exonic splicing regulatory sequences —the complex definition of enhancers and silencers. *Mol. Cell.* **22:** 769–781.
27. Dominski, Z., and R. Kole. 1991. Selection of splice sites in pre-mRNAs with short internal exons. *Mol. Cell. Biol.* **11:** 6075–6083.
28. Hertel, K. J. 2008. Combinatorial control of exon recognition. *J. Biol. Chem.* **283:** 1211–1215.